PET nano-radiotracers for targeted neutrophil detection in pulmonary arterial hypertension

Lucía Fadón-Padilla, Ana Beatriz,, Marta Beraza, Desiré Di Silvo, Ainhize Urkola, María Jesús Sánchez, Irati Aiestaran, Edurne Berra, Susana Carregal and Jesús Ruíz-Cabello

Department of Diagnostic Radiology and Nuclear Medicine, University of Maryland School of Medicine, Baltimore, MD.

Background

Pulmonary arterial hypertension (PAH) courses with remodeling of the pulmonary vasculature and hypertrophy of the right ventricle of the heart. Inflammatory processes, such as neutrophils, are involved in its development and have recently been linked to pathological angiogenesis and vascular dysfunction. Positron emission tomography (PET) with ^{18}F-fluordeoxyglucose (^{18}F-FDG) is widely used to monitor inflammatory processes in PAH and other diseases *in vivo* but lacks cell specificity.

In this study we explored the possibility of using N-cinnamoyl-F-(D)L-F-(cFLFLF) for neutrophil imaging. This peptide is a formylpeptide receptor 1 (FPR1) antagonist. FRP1 is highly expressed on the plasma membrane of neutrophils in response to inflammatory stimuli. We produced ligand-mediated targeted nanoprobes based on IONP-cFLFLF radiolabeled with ^{68}Ga ($t_{1/2}$ = 68 min) for detection of neutrophils in animal models of PAH by PET.

Objective

This study explored the potential of nano-radiotracers based on ultrasmall iron oxide nanoparticles, that were functionalized with the N-cinnamoyl-F-(D)L-F peptide, to detect an increase in neutrophil population in the context of PAH.

Methods

cFLFLF was covalently attached to ultra-small (<5 nm) citrate-coated iron oxide nanoparticles (IONPs) and radiolabeled with ^{68}Ga ($t_{1/2}$ = 68 min)

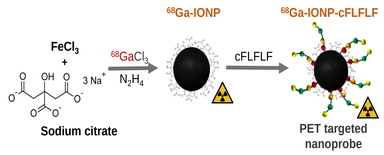

PAH was induced in female Sprague Dawley rats by a single injection of Crotaline (MCT group), or by a single injection of sugen plus 3 weeks of hypoxia (10% 02) (SuHx group).

Three/four weeks after administration, rats were subjected to ^{68}Ga-IONP-cFLFLF and ^{18}F-FDG PET imaging. Magnetic resonance imaging, right ventricular pressure measurements and histological staining were also performed to evaluate evolution of PAH.

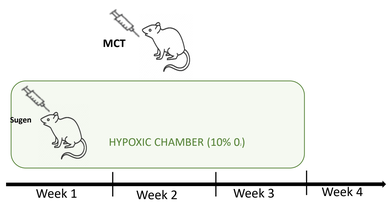

Results

Figure 1. Development of two different PAH animal models: phenotypic characterization.

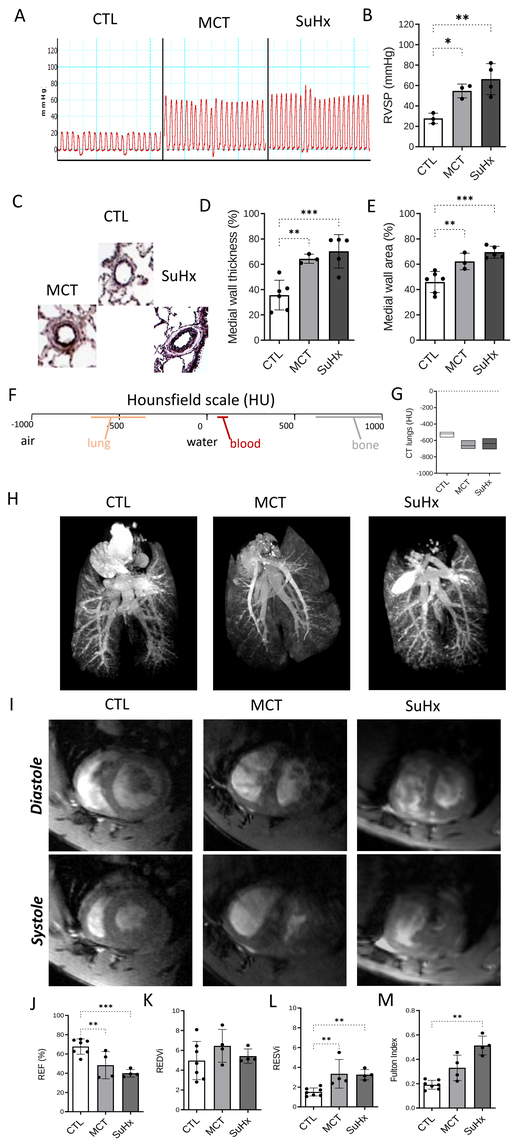

(A) Representative plots of the RVSP values of each animal group. (B) Measurement of right ventricular pressure after disease development. (C) Representative images of each group of elastic staining of arterioles in lung sections. Measurement of vascular remodeling calculating (D) medial wall thickness, and (E) medial wall area. (F) Measurement of the Hounsfield Units (HU) in three VOIs of each lung image acquired by CT. (G) Three-dimensional reconstructions of CT images of the lungs. (H) Diagram of X-ray attenuation of different tissues, quantified as HU. (I) Cross-sectional representative images of the heart of a representative animal of each group acquired by MRI in diastole (top image) and systole (bottom image). Measurement of the right-ventricle ejection fraction (REF, J), the right-ventricle end-diastolic volume index (REDVi, K), the right-ventricle end-systolic volume index (RESVi, L) and the Fulton index (M). Values are presented as mean ± SD, **p-value < 0.01, ***p-value < 0.001 assessed by the One-way ANOVA test.

Figure 2. ^{18}F-FDG PET imaging as a marker for lung inflammation.

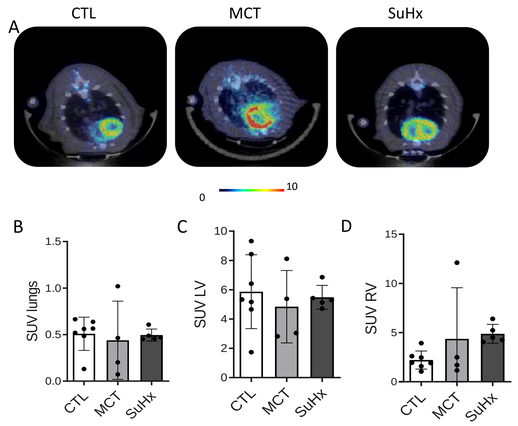

(A) Overlay image of the three-dimensional reconstructions of CT (grayscale) and mid-ventricular axial PET images (color scale represented on the left of the images). Measurement of the standardized uptake value (SUV) in the (B) lungs, (C) LV and (D) RV. Values are presented as mean ± SD assessed by a One-way ANOVA test.

Figure 3. In vivo imaging monitoring of neutrophil infiltration through ^{68}Ga-IONP-cFLFLF.

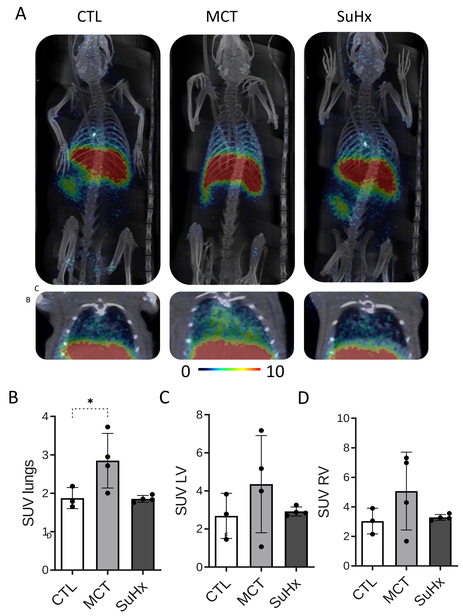

(A) Overlay representation of a representative image of the 3D reconstructions of CT (Maximum Intensity Projection, grayscale) and PET (color scale displayed over the CT images) images, coronal plane. The bottom images correspond to lung sections. Measurement of the standardized uptake value (SUV) in the left-ventricle (SUV LV) (B), right-ventricle (SUV RV) (C), and lungs (SUV lungs) (D). Values are provided as mean ± SD, *p-value < 0.05.

Figure 4. Detection of neutrophils in pulmonary tissue.

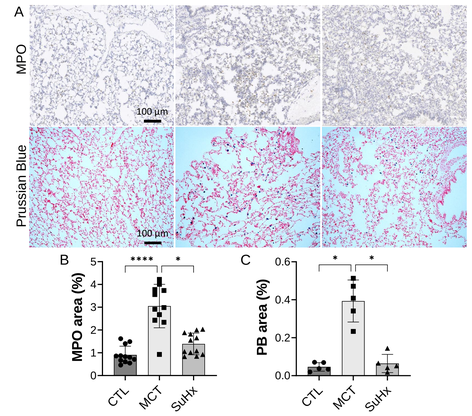

(A) Representative images of lung tissue stained with MPO (neutrophils) and Perls Prussian Blue (iron). (B) Bar graph showing the percentage of MPO (B) and Prussian Blue (C) staining in different regions of interest (ROI) such as the images shown in (A). Values are provided as mean ± SD, *p-value < 0.05, ****p-value < 0.0001.

Conclusions

This study provides promising results regarding the use of ^{68}Ga-IONP-citrate-cFLFLF as a nano-radiotracer for targeted detection of neutrophils and suggest that this nanoprobe can be used to investigate cell-specific inflammatory processes causing the differences observed in RV heart failure and vascular wall remodeling in PAH. Our histological data supports the direct link of neutrophils and nano-radiotracer accumulation in the lung of MCT animals. Overall, the study underscores the importance of imaging in providing individualized and longitudinal evaluations of diseases. The use of nano-radiotracer probes like ^{68}Ga-IONP-citrate-cFLFLF can potentially aid in the diagnosis and monitoring of diseases, as well as in the development of new therapies.

References

Pellico J, Lechuga-Vieco AV, Almarza E, et al. In vivo imaging of lung inflammation with neutrophil-specific ^{68}Ga nano-radiotracer. *Sci Rep*. 2017;7(1):13242. Published 2017 Oct 16. doi:10.1038/s41598-017-12829-y

Park JB, Suh M, Park JY, et al. Assessment of Inflammation in Pulmonary Artery Hypertension by ^{68}Ga-Mannosylated Human Serum Albumin. *Am J Respir Crit Care Med*. 2020;201(1):95-106. doi:10.1164/rccm.201903-0639OC